

Growth of canopy red oak near its northern range limit: current trends, potential drivers, and implications for the future

Rebecca L. Stern, Paul G. Schaberg, Shelly A. Rayback, Paula F. Murakami, Christopher F. Hansen, and Gary J. Hawley

Abstract: Red oak (*Quercus rubra* L.) is projected to expand into the northern hardwood forest over the coming century. We explored the connection between red oak basal area growth and a number of factors (tree age and size, stand dynamics, site elevation, and climate and acid deposition variables) for 213 trees in 11 plots throughout Vermont, USA. Red oak growth generally increased over the course of the chronology (1935–2014) and has been particularly high in recent decades. Growth differed among elevational groups but did not differ between age or size groups. Summer moisture metrics were consistently and positively associated with growth, whereas fall moisture was associated with reduced growth in recent decades. Higher summer temperatures were often negatively associated with growth, though there was evidence that low temperatures in the summer (higher elevations) and fall (lower elevations) constrain growth. Several pollution metrics were associated with reduced growth, a surprising result for a species not known to be sensitive to inputs of acid deposition that have predisposed other species in the region to decline. While red oak growth is currently robust, increases in summer temperatures, reductions in growing season precipitation, or increases in fall precipitation could reduce future growth potential.

Key words: *Quercus rubra*, dendrochronology, tree rings, climate change, acid deposition.

Résumé : Le chêne rouge (*Quercus rubra* L.) devrait augmenter sa présence dans la zone des forêts de feuillus nordiques au cours du prochain siècle. À partir de 213 arbres répartis dans 11 placettes établies dans l'État du Vermont, aux États-Unis, nous avons exploré les liens entre la croissance en surface terrière du chêne rouge et les facteurs suivants: l'âge et la taille des arbres, la dynamique des peuplements, l'altitude de la station, et des variables climatiques et de dépôts acides. La croissance du chêne rouge a généralement augmenté pendant la période couverte par la chronologie (1935–2014) et a été particulièrement élevée au cours des dernières décennies. La croissance était différente entre les classes d'altitude, mais pas entre les classes d'âge ou de taille. Les mesures d'humidité estivale étaient systématiquement et positivement associées à la croissance, tandis que l'humidité automnale était négativement associée à la croissance au cours des dernières décennies. Des températures estivales élevées étaient souvent associées négativement à la croissance, bien que de basses températures estivales (altitudes plus élevées) et automnales (altitudes plus basses) aient aussi limité la croissance. Plusieurs mesures de pollution ont été associées à une réduction de croissance, ce qui est un résultat surprenant pour une espèce qui n'est pas reconnue pour sa sensibilité aux dépôts acides qui ont, par ailleurs, prédisposé d'autres espèces de la région à un déclin. Bien que la croissance du chêne rouge soit actuellement robuste, l'augmentation des températures estivales, la réduction des précipitations pendant la saison de croissance ou l'augmentation des précipitations automnales pourraient réduire son futur potentiel de croissance. [Traduit par la Rédaction]

Mots-clés : *Quercus rubra*, dendrochronologie, anneaux de croissance, changements climatiques, dépôts acides.

Introduction

As climate change progresses, efforts are underway to understand how and when forests and constituent tree species will respond. Numerous studies have applied models to estimate the composition and dynamics of future forests and help in resilience planning (e.g., Gray and Hamann 2013; Iverson et al. 2017; Wang et al. 2017); however, with any model, some fundamental limitations exist in accounting for the future performance of any given species. In particular, empirical evidence is needed to evaluate the fitness and climate response of species projected to experience changes in future suitable habitat.

Areas of noteworthy interest for answering questions around shifting tree performance are transition zones, where different

forest types converge. In the northeastern United States (US), the state of Vermont (VT) is one such area where forest types mix (Cleland et al. 2007). Here, maple–beech–birch forests currently predominate, but climate conditions are projected to shift towards those favoring oak–hickory forests (a forest type that currently provides the greatest total live-tree biomass on US timberland; Oswalt et al. 2014) over time as the climate warms. Indeed, by the year 2100, the oak–hickory forest, which includes northern red oak (*Quercus rubra* L.), is anticipated to gain a significant amount of suitable habitat within the northeastern US under all atmospheric carbon dioxide emission scenarios (Prasad et al. 2007–ongoing). For red oak specifically, increases in growing season (May through September) temperatures are projected to have a particularly strong influence on improving habitat suitability.

Received 5 June 2019. Accepted 19 February 2020.

R.L. Stern, C.F. Hansen, and G.J. Hawley. Rubenstein School of Environment and Natural Resources, University of Vermont, Burlington, VT 05405, USA.

P.G. Schaberg and P.F. Murakami. U.S. Department of Agriculture Forest Service, Northern Research Station, Burlington, VT 05405, USA.

S.A. Rayback. Department of Geography, University of Vermont, Burlington, VT 05405, USA.

Corresponding author: Rebecca L. Stern (email: rstern1@uvm.edu).

This work is free of all copyright and may be freely built upon, enhanced, and reused for any lawful purpose without restriction under copyright or database law. The work is made available under the [Creative Commons CC0 1.0 Universal Public Domain Dedication](https://creativecommons.org/licenses/by/4.0/) (CC0 1.0).

ity in the north (Prasad et al. 2007–ongoing), though this awaits field verification.

Anthropogenic drivers other than climate can also have a detectable influence on tree growth. For example, defoliation from introduced gypsy moth (*Lymantria dispar* (Linnaeus, 1758)) larvae have periodically been associated with significant reductions in radial growth within eastern forests (e.g., Naidoo and Lechowicz 2001), though this has historically had less of an influence in VT (Vermont Department of Forests Parks and Recreation 2019). Acid deposition has also been shown to predispose a number of north-eastern tree species to health and productivity declines (e.g., Kosiba et al. 2018; Schaberg et al. 2001; Schaberg et al. 2010), though detrimental effects on oak growth have not yet been documented (e.g., Levesque et al. 2017; LeBlanc 1998). Furthermore, red oak's ability to expand regionally likely also depends on the legacies of changing land use, including the reduced prevalence of fire that might have favored oak regeneration previously (Nowacki and Abrams 2008).

Numerous factors may differentially impact the growth of red oak within the northern forest. Tree-ring data can provide valuable evidence with its unique ability to document growth data necessary to develop historical relationships between tree growth and climate. With chronologies spanning decades to centuries, tree rings can highlight how these relationships have shifted in accordance with changes in environmental cues, notably climate (Bishop et al. 2015). Moreover, trees near a species' range limit may provide a particularly good indication of possible responses because these populations are often climate sensitive (e.g., Hackett-Pain et al. 2015; Pederson et al. 2004).

Our objective for this study was to identify the climate and potential pollution variables that have been best associated with red oak growth. We measured tree rings for 213 dominant and co-dominant red oak trees at 11 VT sites and statistically compared growth with tree and stand characteristics and regional climate and pollutant deposition data. Because red oak wood is ring-porous, exhibiting a bimodal distribution of vessels (Woodcock 1989), xylem growth can be easily partitioned into earlywood (EW) and latewood (LW) growth, as well as whole ring widths (WRW). A variety of EW vessel parameters (i.e., the width, area, and number of vessels) have been shown to be especially sensitive to different climate factors as compared with measures of LW or WRW (e.g., Tardif and Conciatori 2006a). Therefore, we evaluated relationships between WRW, LW, and EW growth and environmental factors that may influence growth. Overall, we hypothesized that

(H₁) growth will be positively related to growing season temperature (mean, minimum, and possibly maximum) because sampled populations are near the northern edge of the species' range (Burns and Honkala 1990);

(H₂) growth will be positively related to moisture variables because the species is vulnerable to catastrophic xylem embolism (Cochard and Tyree 1990);

(H₃) growth will not be related to sulfur and nitrogen deposition inputs because red oak is not known to be sensitive to acid deposition (LeBlanc 1998); and

(H₄) growth response will differ little based on tree and site characteristics (e.g., tree age, size, and stand elevation) because most sites likely originated during a similar period of agricultural land abandonment (Foster 1992) and because oak occupy a relatively uniform elevational band within VT (Gudex-Cross et al. 2019).

Methods

Study area

The study area is located in western VT, ranging in latitude from 42.75°N to 44.82°N and in longitude from 73.02°W to 73.24°W (Fig. 1), situated in the western valleys of the Green Mountains. Mean temperature (1935–2014) is warmest in July (19.5 °C) and coldest in January (−8.5 °C); mean annual precipitation is 108 cm, with 48% of precipitation falling from May through September (Fig. 2; NOAA National Climatic Data Center 2018). Over the past century in this region, both temperature and total annual precipitation have increased (Janowiak et al. 2018). Within this area, 11 second-growth forest stands at varying elevations that have recovered from intensive land use in the early 20th century were selected for study. Soils at the 11 sites are loamy or coarse-loamy, derived from glacial till (Soil Survey Staff, Natural Resources Conservation Service, United States Department of Agriculture 2019). We were not selective in choosing sites with specific intrinsic characteristics such as aspect, soil type, or elevation; rather, we were interested in choosing sites that would provide a broad representation of mature red oak trees in the northern part of the species' range. We avoided areas with a known history of management over the past several decades, because human disturbance can influence and obscure other potential drivers of growth (e.g., climatic or pollutant). In addition to red oak, other deciduous tree species at these sites included *Quercus alba* L., *Fagus grandifolia* Ehrh., and *Acer rubrum* L., and coniferous species included *Pinus strobus* L. and *Tsuga canadensis* (L.) Carrière.

Dendrochronological techniques

The goal of this study was to assess the possible sensitivities of red oak growth to climate and pollution factors in the species' northern range. To better isolate environmental signals in this species, we focused on sampling dominant and co-dominant trees rather than conducting a complete ecological analysis that included intermediate and suppressed trees. The growth of intermediate and suppressed trees would include trends such as those related to competition, which could obscure the environmental signals that we were seeking to understand. Thus, to detect the influence of the environmental factors on red oak growth, we collected increment cores only from dominant and co-dominant red oak trees ($n = 213$) following standard dendrochronological techniques (Stokes and Smiley 1968). Two xylem increment cores (5 mm in diameter) were collected from each tree at breast height (1.37 m above ground level), 180° from each other and perpendicular to the slope. Between 15 and 20 trees were cored per site for all but three sites (Supplementary Table S1).¹ Trees with observable bole or crown damage were avoided to better characterize mean growth and minimize the influence of nonclimatic factors on growth.

Following collection, cores were oven-dried, mounted, and sanded with progressively finer grit sandpaper (ranging from 220 to 800 grit). Annual whole-ring increments were visually cross-dated using the list method (Yamaguchi 1991) and microscopically measured to 0.001 mm resolution using a Velmex sliding stage unit (Velmex Inc., Bloomfield, NY, USA) with MeasureJ2X v. 5.05 software (VoorTech Consulting, Holderness, N.H., USA). EW and LW widths were also visually partitioned and measured, as EW is composed of visibly larger vessels (García-González et al. 2016). The program COFECHA v. 6.06 was used to statistically detect and correct for cross-dating errors in the whole-ring series (Holmes 1983). Dendrochronological statistics such as series intercorrelation, autocorrelation, and average mean sensitivity (but see Bunn et al. 2013) were determined, and the expressed population signal (EPS) was calculated based on the equation presented by Wigley et al. (1984). EPS

¹Supplementary data are available with the article through the journal Web site at <http://nrcresearchpress.com/doi/suppl/10.1139/cjfr-2019-0200>.

Fig. 1. Locations of the 11 red oak sites throughout Vermont, delineated by elevational group (▲, higher elevation (≥ 258 m); ●, lower elevation (< 258 m)). Inset shows historical range map and field inventory analysis importance value data (Prasad and Iverson 2003), indicating red oak's dominance in a given forest area. Figure was created using ArcGIS 10. Base map courtesy of Esri, USGS, and NOAA.

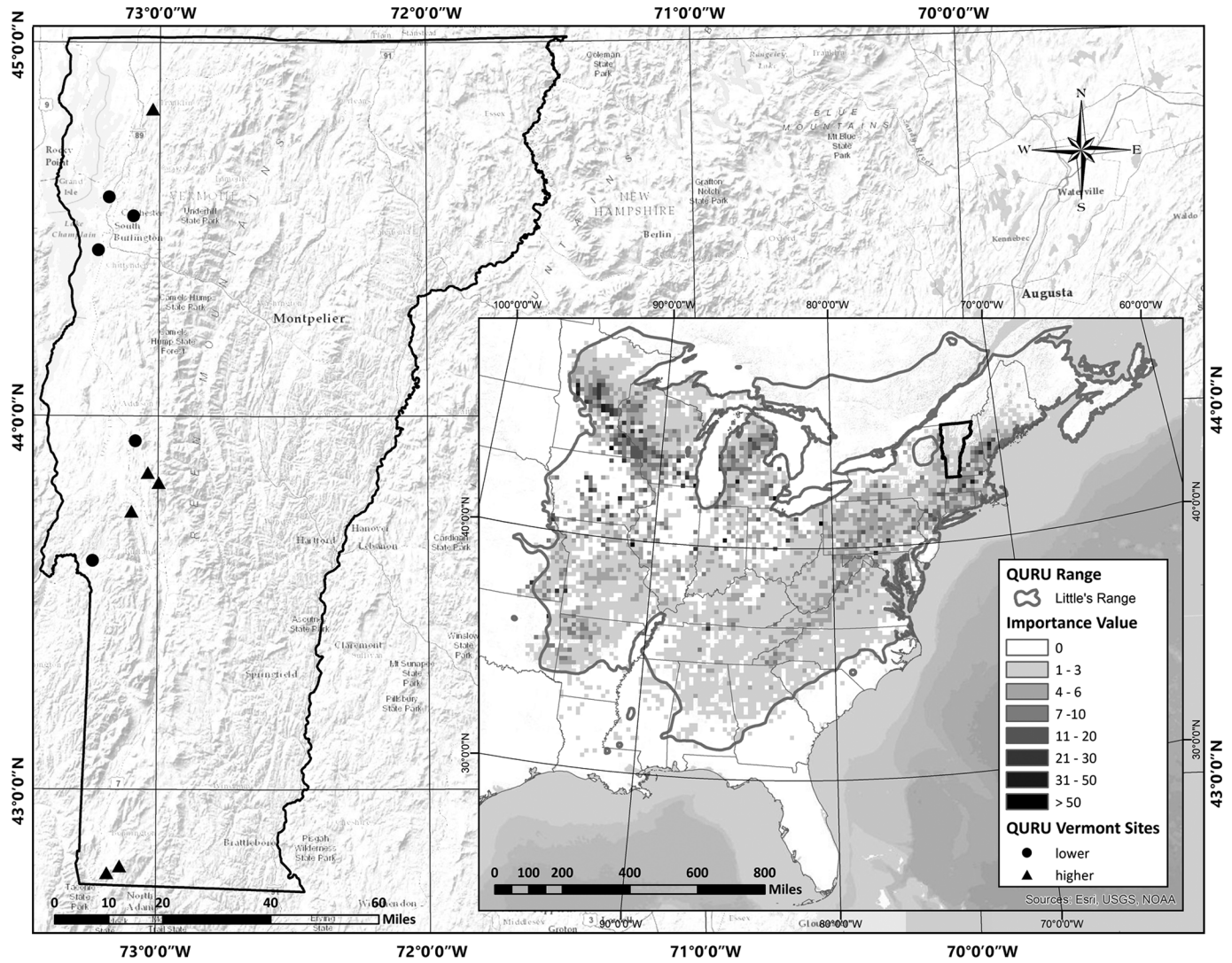
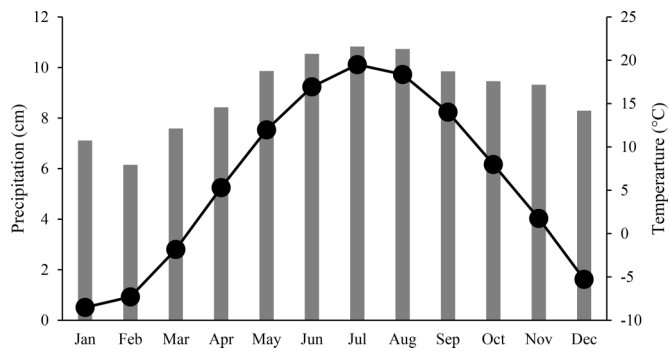


Fig. 2. Monthly mean temperature (black circles) and monthly total precipitation (grey bars) for the study area from 1935 to 2014 (NOAA National Climatic Data Center 2018).



values (cutoff of 0.80) determined the time period (1935 onward) over which all plot chronologies maintained a robust stand-wide signal (but see Buras 2017). Individual cores were occasionally discarded from a site chronology if they correlated poorly with the master chronology (i.e., below Pearson critical correlation 99%

confidence levels) due to unusual growth trends that were not representative of overall site growth. Approximate tree age at breast height was calculated using the maximum number of rings per tree if the pith was evident. If the pith was not visible, core age was estimated using a pith estimator (Speer 2010) based on the curvature of the innermost annual rings. Age was not assessed for incomplete cores that did not exhibit ring sequence curvature.

Statistical analyses

To determine if any stand-wide release events occurred over the period of the chronologies, individual tree growth (raw ring width, RRW) was analyzed per plot using the radial-growth averaging criteria established by Nowacki and Abrams (1997). A 10-year running median with a 50% threshold was employed to detect major release events, with a stand-wide release defined as $\geq 25\%$ of the trees experiencing a major release within the same decade (Nowacki and Abrams 1997). Release events were discerned using the TRADER package for R (function growthAveragingALL; Altman et al. 2014).

RRW measurements for both cores were averaged per tree and standardized using two methods. Standardization creates a dimensionless index by dividing the observed ring widths by the expected value of a detrended chronology (Fritts 1976). We first

Can. J. For. Res. Downloaded from www.nrcresearchpress.com by USDANALBF on 10/02/20 For personal use only.

calculated basal area increment (BAI), which converts diameter increments ($\text{cm}\cdot\text{year}^{-1}$) into area increments ($\text{cm}^2\cdot\text{year}^{-1}$) to minimize age–size growth trends (West 1980). BAI chronologies were calculated per site and across all sites to create a study-wide chronology (functions `bai.out` and `chron` in R package `dpLR`; Bunn et al. 2016). For our second RRW standardization, we created ring width indices (RWIs) using a 67% n cubic smoothing spline with a 50% frequency response cutoff using the `detrend` function in the R package `dpLR` (Bunn et al. 2016). We chose this spline method because it removes low-frequency variance and smooths out the growth trends considered noise (e.g., the result of stand-wide release events) while leaving in climate signals (Cook and Peters 1981). Autoregressive modeling was performed on the standardized series to reduce the influence of endogenous disturbances, remove the effects of temporal autocorrelation (first-order autocorrelations), and enhance the common signal (Cook 1985), resulting in prewhitened (residual) chronologies. We utilized residual chronologies because through detrending, standardizing, and prewhitening, this type of chronology removes the most disturbance related growth, and the remaining interannual variance can be related to exogenous factors (Cook and Peters 1997; Cook 1985). Annual mean values of growth were computed using Tukey's biweight robust mean, which minimizes the effect of outliers (Cook and Kairiukstis 1990) and increases the common signal. Residual RWI chronologies were calculated per site, across all sites to create a state-wide chronology, and then truncated to the common period of 1935 to 2014 based on EPS results. A mean RWI chronology was calculated for WRW and was also developed for EW and LW growth, as these portions of woody growth can be sensitive to different climatic drivers (García-González et al. 2016).

Climate and pollutant deposition data

A wide range of climatic variables were evaluated for possible associations with red oak growth (Supplementary Table S2).¹ To evaluate moisture variables, data from the standardized precipitation–evapotranspiration index (SPEI) were obtained for individual sites and averaged to create a state-wide SPEI dataset at four time steps (Supplementary Table S2¹; Vicente-Serrano et al. 2017). SPEI is a moisture index that accounts for precipitation and potential evapotranspiration in estimating drought and includes the impact of increasing temperatures on water demand (Vicente-Serrano et al. 2010). Only the 1- and 3-month time steps (SPEI01 and SPEI03, respectively) were used for further analyses. These variables have less temporal memory compared with SPEI06 and SPEI09 and can also highlight the importance of an entire season (SPEI03) or point to the significance of a specific period within a season (SPEI01). Similarly, although direct precipitation data were also initially assessed, they were not used in final analyses because they were not independent of the more ecologically significant SPEI measures. A total time span for the climate and SPEI datasets of 1934–2014 was selected to match that of the tree-ring data.

To evaluate temperature variables, we acquired climate data from the National Climatic Data Center (NOAA National Climatic Data Center 2018) for VT Climate Division 2 (Western Division), because our sites spanned this division's latitudinal gradient. As we were interested in identifying a broad climate signal across all sites, climate division data were used to provide more uniform variables that could be interpreted beyond the individual site level. We focused on two variables to reduce redundancy and intercorrelation of climatic data: monthly maximum temperature (T_{max}) and monthly minimum temperature (T_{min}), from which we also created seasonal (winter, December–February; spring, March–May; summer, June–August; fall, September–November) and water-year (Wyr, previous October – current September) metrics. We also assessed two heat indices: heating degree days (HDD) and cooling degree days (CDD). HDD is a gauge of low-temperature exposure calculated as the number of degrees that a day's mean temperature is below $18.3\text{ }^{\circ}\text{C}$ ($65\text{ }^{\circ}\text{F}$). Conversely,

CDD is a measure of high-temperature exposure calculated as the number of degrees that a day's mean temperature is above $18.3\text{ }^{\circ}\text{C}$ ($65\text{ }^{\circ}\text{F}$). Although HDD and CDD were devised for evaluating building heating and cooling requirements, they have been shown to also relate to tree growth and physiology and can be used as proxies for higher or lower temperature exposure over time (e.g., Kosiba et al. 2018).

Pollutant deposition data (SO_4^{2-} , NO_3^- , cation-to-anion ratio, and rainfall pH) were obtained from two sources: two National Atmospheric Deposition Program (National Atmospheric Deposition Program 2017) sites in VT (Underhill and Bennington) and the Hubbard Brook Ecosystem Study in New Hampshire (Likens 2016). Data from the two VT sites (1982–2014) were averaged and then regressed against deposition data from New Hampshire (1965–2012) to extend the VT data back from 1982 to 1965. The resulting total time span used for the combined dataset was 1974–2014 (Supplementary Table S2),¹ which corresponded with the second half of the chronology.

Correlations and model building

Stationary correlation functions were calculated using Pearson's correlations (function `dcc`, R package `treeclim`; Zang and Biondi 2015) using bootstrap resampling (1000 bootstrap samples; Biondi and Waikul 2004). Correlations were conducted between monthly, seasonal, and Wyr climate data and the extent of the regional RWI chronologies (1935–2014), spanning an 18-month window from the previous year's June to the current year's November, to allow us to explore the effect of the previous year's climate and pollution deposition on the following year's growth. To evaluate potential changes in significant correlations over time, we also conducted moving correlation functions with a window of 25 years for the same set of variables (R package `treeclim`; Zang and Biondi 2015). In addition, because deposition data were not available for the entire chronology, we were able to assess the influence of pollution on growth during the second half of the chronology (1975–2014). Correlations were calculated with monthly, seasonal, and Wyr pollution deposition data.

Significant correlation variables were then utilized to build a series of plausible models for the entire tree-ring chronology (1935–2014), using a generalized linear model approach with Gaussian distribution. For model inputs, we only used variables with a correlation $\alpha = 0.01$ to limit the number of significant variables, reduce redundancy, and focus on the most powerful relationships. A null model (intercept only) was built to serve as a benchmark for comparing relative model fit with an uninformed model. Pollution deposition variables were not included in models as data were not available for the entire time period.

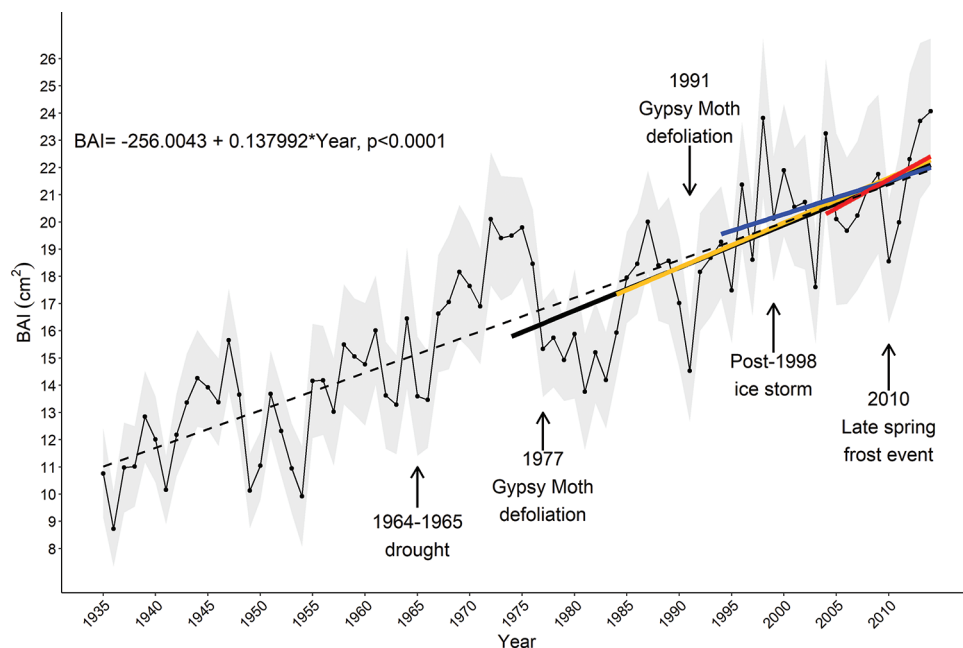
Models were assessed for multicollinearity using variance inflation factors (VIF; Marquardt 1970) by applying the function `vif` in the R package `car` (Fox and Weisberg 2011). Models with a high VIF (>2) were removed. From the remaining models with $\text{VIF} < 2$, the model with the lowest Akaike's information criterion (AIC; Akaike 1974) was selected. When ΔAIC between models was <2 , the most parsimonious one was chosen. P values, which identify the significance of each model by comparing the reduced deviance between the null and candidate models, were computed using an analysis of variance (ANOVA) with an F distribution. Adjusted R^2 was calculated as the squared correlation between predicted and observed values.

Results

General growth trends: BAI and RWI

Across all 11 sites, red oak trees had an estimated median age range of 83–149 years and a mean diameter at breast height (DBH) range of 32.2 to 55.3 cm (Supplementary Table S1).¹ One site (Castleton) exhibited a stand-wide release event of unknown origin in 1954–1964. From 1935–2014, red oak growth (BAI) generally

Fig. 3. Mean basal area increment (BAI) growth (\pm SE) from 1935 to 2014 for red oak trees at 11 sites located throughout Vermont. The linear regression of growth over time (dotted line and the associated equation) is presented, as are known regional stress events (Vermont Department of Forests Parks and Recreation 2019) that were identified at the time of occurrence. Linear trend lines for the last 10 (red), 20 (blue), 30 (yellow), and 40 (black) years are shown as well.



increased ($P < 0.0001$), with maximum growth in 2014 at 26.2 cm^2 (Fig. 3). Temporary reductions in growth were evident after multiple regional stress events: drought in 1964 and 1965 (NOAA National Centers for Environmental Information 2018); gypsy moth defoliations in 1977 and 1991; the 1998 ice storm; and a late spring frost event in 2010 (Vermont Department of Forests Parks and Recreation 2019). Sites were partitioned into two approximately equal groups based on mean tree size (44.3 cm), median age (102 years), and median elevation (258 m). Regarding tree size and age, there was no difference in BAI slope over time for stand-level chronologies (1935–2014); however, there was a difference in statistical slope between elevation groups: lower elevation ($<258 \text{ m}$) sites showed a greater rate of increased growth over the length of the chronology than red oak sites at higher elevations ($>258 \text{ m}$; $t = 2.47$, $P = 0.04$).

Chronology curves for WRW and LW (Fig. 4) were very similar ($r = 0.98$), suggesting that yearly variations in WRW may have arisen from changes in LW growth. The EW chronology exhibited considerably less year-to-year variability than WRW or LW growth ($r = 0.29$ and $r = 0.15$, respectively).

Climate–growth and deposition–growth correlations

Patterns for WRW, EW, and LW chronologies

Moisture-related variables during the summer months were consistently associated with red oak growth (Fig. 5). For the 1935–2014 period, June and July SPEI01 ($r = 0.40$ and $r = 0.36$, respectively; $P \leq 0.01$) were significantly related to WRW growth. Seasonal summer moisture variables were also important metrics: SPEI03 for June, July, and August ($r = 0.32$, 0.41 , and 0.34 , respectively; $P \leq 0.01$). In addition to moisture variables, June T_{max} showed a negative correlation with growth ($r = -0.39$, $P \leq 0.01$), as did June CDD, a measure of accrued heat ($r = -0.27$, $P \leq 0.01$; Fig. 6). June HDD, a measure of accumulated cold, exhibited a positive correlation with WRW ($r = 0.26$, $P \leq 0.01$), highlighting the same influence of temperature (Fig. 6). WRW showed a negative correlation (1975–2014) with July SO_4^{2-} ($r = -0.29$, $P \leq 0.05$; Fig. 5). The LW chronology exhibited similar patterns to the WRW chronology, but with generally stronger correlations and three additional correlations with SO_4^{2-} (1975–2014): previous November ($r = -0.25$,

$P \leq 0.05$), June ($r = -0.30$, $P \leq 0.05$), and summer ($r = -0.26$, $P \leq 0.05$; Fig. 5).

EW was far less variable over time than WRW or LW chronologies (Fig. 4). Still, even this more uniform architectural component displayed variability related to climate. The EW chronology was positively correlated with SPEI01 for the previous July ($r = 0.31$, $P \leq 0.01$) and SPEI03 for the previous August and September ($r = 0.32$ and 0.38 , respectively; $P \leq 0.01$; Fig. 5).

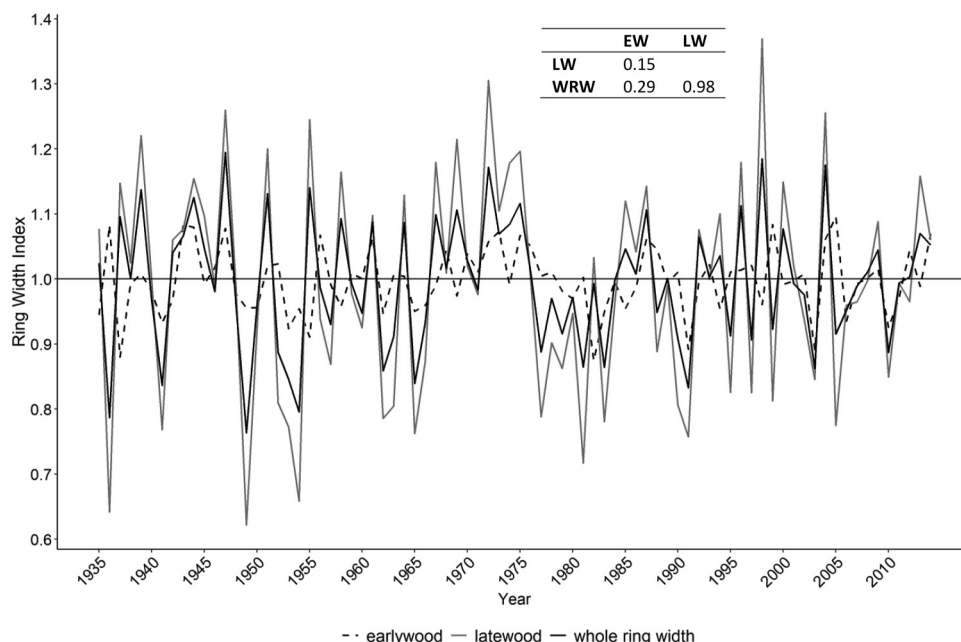
WRW patterns based on elevation

To understand how climate response may vary among sites, we compared climate–growth and deposition–growth correlations between lower and higher elevation sites (Figs. 7, 8, 9). Certain correlations highlighted differences between the elevational groupings: growth (1935–2014) at low-elevation sites was negatively correlated with HDD from the previous October ($r = -0.28$, $P \leq 0.01$), and growth at high-elevation sites was positively correlated with T_{min} from August ($r = 0.28$, $P \leq 0.01$). Growth (1975–2014) at low-elevation sites showed a greater sensitivity to pollution parameters than at high-elevation sites (Fig. 9). Low-elevation growth included negative correlations with NO_3^- from April ($r = -0.34$, $P \leq 0.01$), SO_4^{2-} from June ($r = -0.32$, $P \leq 0.01$), and the cation-to-anion ratio from the previous September ($r = 0.29$, $P \leq 0.01$).

Changes in WRW patterns through time

Moving climate–growth correlations highlighted additional significant correlations in recent decades. For example, while only T_{max} from June was significant for the whole chronology, starting in the mid-1970s, T_{max} from July (r value ranging from -0.30 to -0.54 ; $P \leq 0.01$) and summer (r value ranging from -0.51 to -0.67 ; $P \leq 0.05$) were also significant (Fig. 10). HDD, which exhibited significant negative correlations with growth in the beginning of the chronology, were characterized by the opposite sign starting in the mid-1970s (r value ranging from 0.32 to 0.41 ; $P \leq 0.05$; Fig. 10). A new relationship emerged as significant during the mid-1970s as well: a negative correlation with fall moisture (October SPEI03, r value ranging from -0.24 to -0.50 ; November SPEI03, r value ranging from -0.21 to -0.60 ; $P \leq 0.05$).

Fig. 4. Ring width index (RWI) of red oak earlywood (EW), latewood (LW), and whole ring width (WRW) across all 11 Vermont sites. Inserted table shows correlation coefficients between each of the three chronologies.



Growth models

All moisture predictors exhibited a positive relationship with growth, while temperature displayed a negative relationship with growth (Table 1). Based on AIC, the model for 1935–2014 that performed best included summer moisture (July SPEI03) and June T_{\max} ($F = 14.277$, $P < 0.0001$). For a complete listing of the candidate models assessed, see Supplementary Table S3.¹

Discussion

Climate–growth relationships

Red oak has been growing well throughout VT, reaching its highest level of growth during the most recent decades. This BAI trend describes growth for dominant and co-dominant red oak, which could overestimate growth for intermediate and suppressed trees (Nehrbass-Ahles et al. 2014). This evidence of a sustained rise in growth throughout the chronology is, however, in agreement with studies that have observed increasing growth trends into late stand development for several species, including northern red oak trees in the canopy (Foster et al. 2014), and across various age classes (Johnson and Abrams 2009). Summer moisture parameters were some of the most important environmental variables correlated with red oak growth: June and July SPEI01, and general summer moisture (June, July, and August SPEI03). Indeed, the highest overall correlation for the entire chronology span (1935–2014) was July SPEI03 ($r = 0.41$, $P \leq 0.01$). The importance of moisture availability to growth would be expected for a species adapted to conduct large volumes of water through its EW vessels (Zimmerman 1983). Our results concur with findings from red oak in the southeastern US (Pan et al. 1997; Speer et al. 2009), southern Quebec (Tardif and Conciatori 2006b; Tardif et al. 2006), and elsewhere in eastern North America (LeBlanc and Terrell 2011), although drivers of growth can differ based on latitude (Crawford 2012; Martin-Benito and Pederson 2015).

Although less numerous than associations with moisture, negative correlations with maximum summer temperatures and June CDD were evident. As correlations with moisture featured so prominently overall, our observed negative temperature–growth correlations may point to a drought signal. Throughout eastern North America, drought has been found to be the largest climate signal among eight deciduous species (Martin-Benito and Pederson

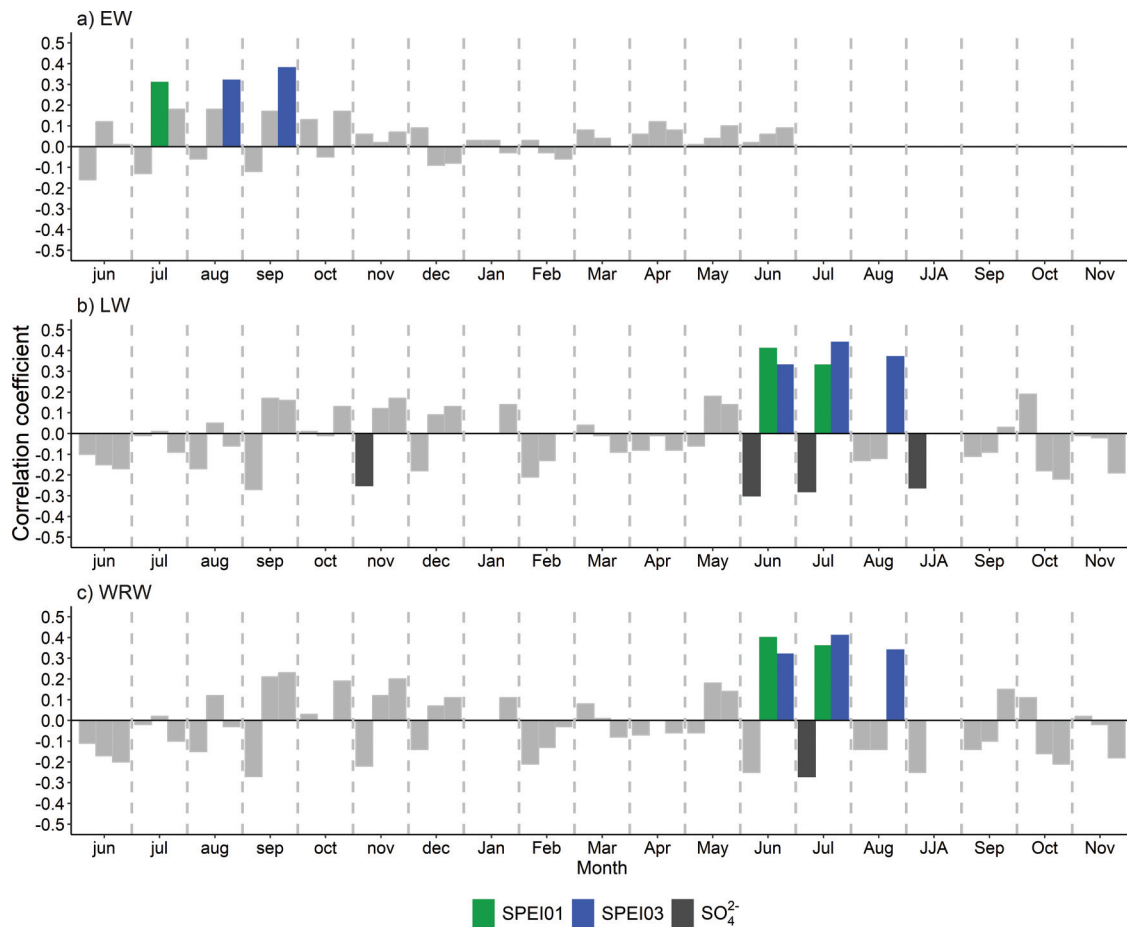
2015), though of all species sampled, red oak exhibited the weakest link with precipitation. Moreover, drought has been shown to be a significant driver of tree growth among 24 species in eastern North America, including red oak (D’Orangeville et al. 2018). Additional findings suggest that moisture has been a driving factor in tree migration for multiple oak species that have migrated westward along precipitation gradients (Fei et al. 2017).

While higher temperatures drive a more moisture-limited environment, it is also possible that red oak is sensitive to high-temperature exposure directly. On hot days, trees must balance the possibility of xylem embolism with the need to assimilate carbon, especially ring-porous species such as oaks with large-diameter EW vessels that are particularly prone to embolism (e.g., Cochard and Tyree 1990). In an effort to prevent cavitation during hot summer months, red oaks can reduce water loss by decreasing stomatal conductance, which limits carbon dioxide uptake (Cowan and Farquhar 1977) and reduces photosynthesis and growth (Tyree and Cochard 1996). The positive correlation with June HDD further suggests that red oak growth can benefit from moderate-to-cool temperatures (and associated reductions in transpirational water loss) that likely optimize leaf function and carbon capture. In contrast, negative correlations between July HDD and growth were found in the earlier decades of the chronology.

Correlations of LW growth and climate parameters mirror those for WRW (Figs. 5 and 6) and highlight the importance of moisture and moderate temperatures to wood production, especially in LW production that varies more over time. In contrast, EW growth was solely related to the previous year’s moisture metrics, indicating that previous years’ water availability appears to be influential in driving EW growth. These results are in line with Tardif and Conciatori (2006a) who found significant positive correlations between red oak EW and the previous year’s summer moisture indicators in southern Quebec. EW vessels begin to form prior to budbreak (e.g., Kitin and Funada 2016; Takahashi et al. 2013), so their production relies heavily on carbon storage from the previous year (Barbaroux and Bréda 2002), a crucial reserve, as EW vessels are responsible for over 90% of water transport during the growing season (Ellmore and Ewers 1985).

Our models suggest that the influence of intensifying mean summer temperatures in recent decades, whether directly or

Fig. 5. Significant moisture–growth (1935–2014) and deposition–growth (1975–2014) (ring width index) correlation coefficients for (a) earlywood (EW), (b) latewood (LW), and (c) whole ring width (WRW). Lowercase letters indicate previous year's months. Grey bars indicate nonsignificant correlations. Climate–growth correlations were significant at the $P \leq 0.01$ level, while deposition–growth correlations were significant at $P \leq 0.05$. No correlations are shown for current year July thru November for EW, as this wood type has completed growth by this point in the year. JJA, June, July, and August grouped to create a summer variable; SPEI01 and SPEI03, standardized precipitation–evapotranspiration index at 1- and 3-month time steps, respectively; SO_4^{2-} , sulfate deposition. See Methods for more information on variables.



through a consequential decrease in water availability, may impose a greater influence on red oak growth in the future. Starting in the mid-1970s, growth was correlated with not only June T_{\max} , but also July T_{\max} and summer T_{\max} , suggesting that overall warmer summer temperatures — or associated increases in evaporative demand — may be having a greater impact on growth in recent years. In addition, cooler summers in recent decades are associated with increased growth, as evidenced by positive correlations with August HDD during the past 40 years. Alternatively, the northeastern US is experiencing an ongoing pluvial event (Pederson et al. 2013), suggesting that the increase in rainfall may have caused temperature to become the more limiting factor in recent decades.

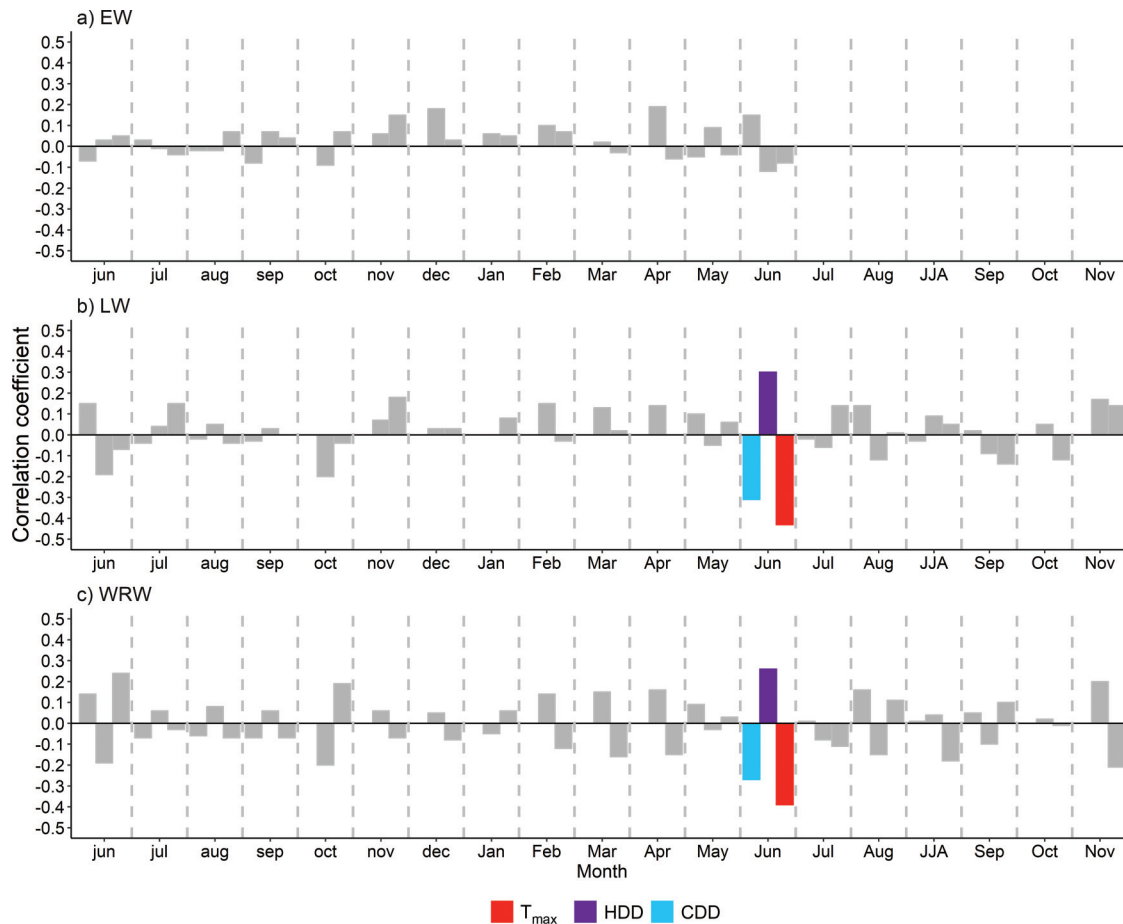
Our findings on drivers of red oak growth overlap with results reported by the Climate Change Tree Atlas (CCTA), which ranks the most important factors that describe future habitat suitability for tree species in the US (Prasad et al. 2007–ongoing). Annual precipitation is an important predictor of red oak habitat in the CCTA, though not specific to the months and seasons that we found to be significant. Mean May–September temperature and mean July temperature are also key predictors of suitable habitat for red oak throughout its range in the CCTA. Elevation, another red oak habitat predictor in the CCTA, featured prominently in our findings as well; low-elevation stands appeared more responsive to moisture and pollution deposition levels, whereas

high-elevation plots appeared more sensitive to temperature. Additionally, the CCTA finds multiple soil factors influential for defining red oak suitable habitat. We explored possible links between similar soil parameters (e.g., available water capacity and depth to bedrock) and xylem growth for our study sites; however, with our sample size and the coarseness of available soil data, there were few apparent differences in soil characteristics among our 11 sites to compare with growth. It is possible that with finer scaled soil data and a larger sample size, soil factors may also be identified as significant modifiers of red oak growth in the region, as soil factors have been found to be a factor in drought responses of trees (Kannenberg et al. 2019).

Pollution deposition–growth correlations

The influence of pollution deposition on growth was evident as negative correlations between SO_4^{2-} inputs on WRW and especially LW growth (Fig. 5). Deposition–growth correlations (evident as relationships with SO_4^{2-} , NO_3^- , pH, and cation-to-anion ratio of rainfall) also differed by elevational group (Fig. 9). Notably, low-elevation red oak sites displayed a number of significant correlations with deposition, while high-elevation sites did not show any. Pollutant deposition has previously been documented as being detrimental to the growth of other tree species in the Northeast — notably red spruce (*Picea rubens* Sarg.) and sugar maple (*Acer saccharum* Marsh.; Schaberg et al. 2001; Schaberg et al. 2010), but it

Fig. 6. Significant temperature–growth (ring width index) correlation coefficients (1935–2014) for (a) earlywood (EW), (b) latewood (LW), and (c) whole ring width (WRW). Lowercase letters indicate previous year's months. Grey bars indicate nonsignificant correlations. JJA, June, July, and August grouped to create a summer variable. Climate–growth correlations were significant at the $P \leq 0.01$ level. No correlations are shown for current year July thru November for EW as this wood type has completed growth by this point in the year. T_{\max} , maximum monthly temperature; HDD, heating degree days; CDD, cooling degree days. See Methods for more information on variables.



was unexpected to find these results for red oak. Additionally, we would normally anticipate higher elevation sites to exhibit a greater sensitivity to pollutant deposition (Lovett 1994), in part because pollution inputs generally increase with elevation. In considering why low-elevation red oak sites appeared more responsive to pollution deposition variables, it is useful to recall that our study sites — including our higher elevation sites (and most oak locations in VT; Gudex-Cross et al. 2019) — would in most contexts be considered low-elevation sites as the highest one was only at 354 m. It is unlikely that deposition levels would be significantly different at the limited range of elevations that we sampled. One possibility for why we found significant correlations with pollutant factors at low-elevation sites is because, generally, these sites were growing at a higher rate (Supplementary Fig. S1).¹ A higher growth rate implies fewer constraints on growth at low-elevation sites; thus, other limitations such as pollution inputs at these locations may better explain growth. As correlations with deposition existed during both summer and fall months (Fig. 9), it seems likely that pollution deposition not only affected tree leaves during the growing season, but also had longer lasting impacts on productivity through shifts in soil acidity and nutrient availability as noted for the region (Driscoll et al. 2001). Although sulfate emissions have declined in the northeastern US over the past several decades (e.g., Siemion et al. 2018) and soils in the Northeast are showing some evidence of improvement (Lawrence et al. 2015), broader recovery will likely be spa-

tially (Lawrence et al. 2015; Siemion et al. 2018) and temporally heterogeneous — taking many decades for the most impacted sites to rebound from chronic acidification and nutrient loss (Driscoll et al. 2001; Likens et al. 1996). In addition, although it has generally decreased over the past 15 years, nitrogen pollution has not significantly decreased in the US in the same way as sulfur (Driscoll et al. 2003), so its deleterious effects are still evident (Greaver et al. 2012). This continued nitrogen loading could explain the negative correlation in our study between growth and Wyr nitrate emissions. Therefore, the observed links with pollution deposition could reflect the legacy of pollution in the region and may result in red oak trees failing to reach their full growth potential in impacted areas.

Implications for future growth

The Northeast region is expected to continue to experience increases in both temperature and precipitation throughout the 21st century (Janowiak et al. 2018). A projected increase in future temperatures must also be considered within the context of the amount of precipitation that falls within any one growing season, and the timing at which precipitation occurs, even if it is increasing. Simulations show that projected increases in summer temperatures over a longer growing season will result in higher potential evapotranspiration rates (Thibeault and Seth 2014), which could add further stress to trees, especially as precipitation increases will largely be driven by late winter and early spring

Fig. 7. Significant climate–growth (1935–2014) correlation coefficients for (a) high-elevation (>258 m) and (b) low-elevation (<258 m) groups. Lowercase letters indicate previous year’s months. Grey bars indicate nonsignificant correlations. All significant correlations are at the $P \leq 0.05$ level unless denoted by an asterisk (*), which indicates significance at the $P \leq 0.01$ level. SPEI01 and SPEI03, standardized precipitation–evapotranspiration index at 1- and 3-month time steps, respectively. See Methods for more information on variables.

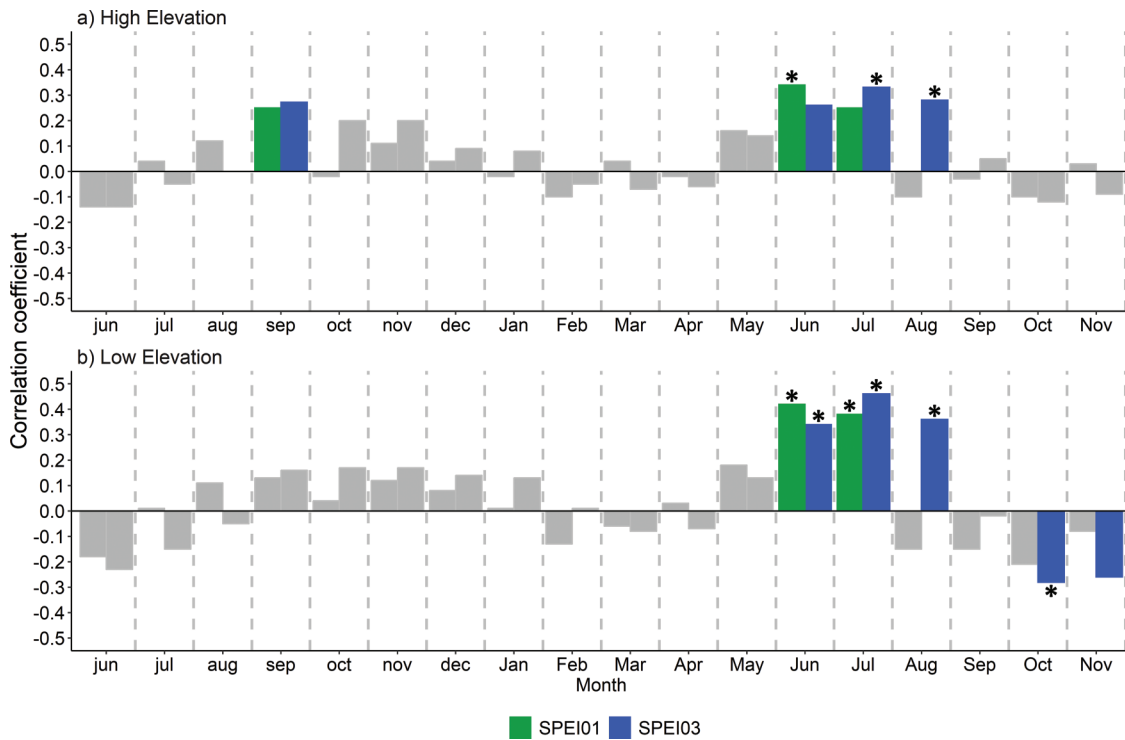
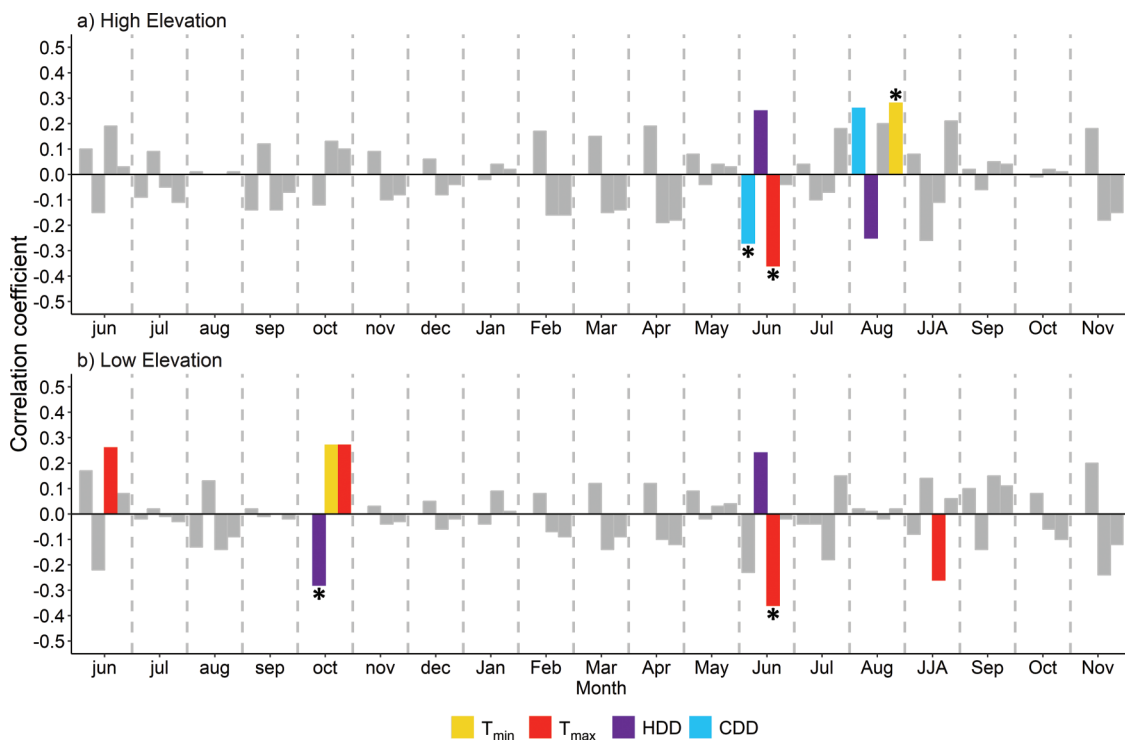
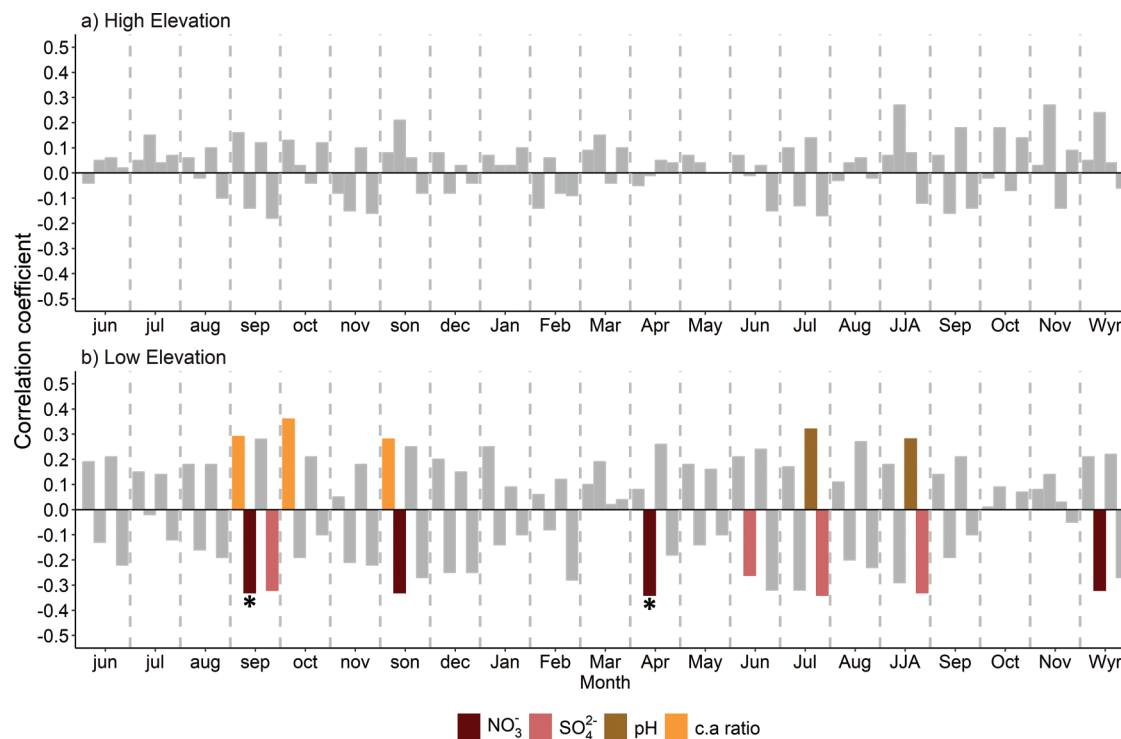


Fig. 8. Significant climate–growth (1935–2014) correlation coefficients for (a) high-elevation (>258 m) and (b) low-elevation (<258 m) groups. Lowercase letters indicate previous year’s months. Grey bars indicate nonsignificant correlations. All significant correlations are at the $P \leq 0.05$ level unless denoted by an asterisk (*), which indicates significance at the $P \leq 0.01$ level. JJA, June, July, and August grouped to create a summer variable; T_{min} , minimum monthly temperature; T_{max} , maximum monthly temperature; HDD, heating degree days; CDD, cooling degree days. See Methods for more information on variables.



Can. J. For. Res. Downloaded from www.nrcresearchpress.com by USDANALBF on 10/02/20 For personal use only.

Fig. 9. Significant deposition–growth (1975–2014) correlation coefficients for (a) high-elevation (>258 m) and (b) low-elevation (<258 m) groups. Lowercase letters indicate previous year’s months. Grey bars indicate nonsignificant correlations. All significant correlations are at the $P \leq 0.05$ level unless denoted by an asterisk (*), which indicates significance at the $P \leq 0.01$ level. JJA, June, July, and August grouped to create a summer variable; son, previous September, October, and November grouped to create a previous fall variable; Wyr, water year for previous October to current September; NO_3^- , nitrate deposition; SO_4^{2-} , sulfate deposition; c.a ratio, cation-to-anion ratio. Note that deposition variables are only significant at lower elevation sites.



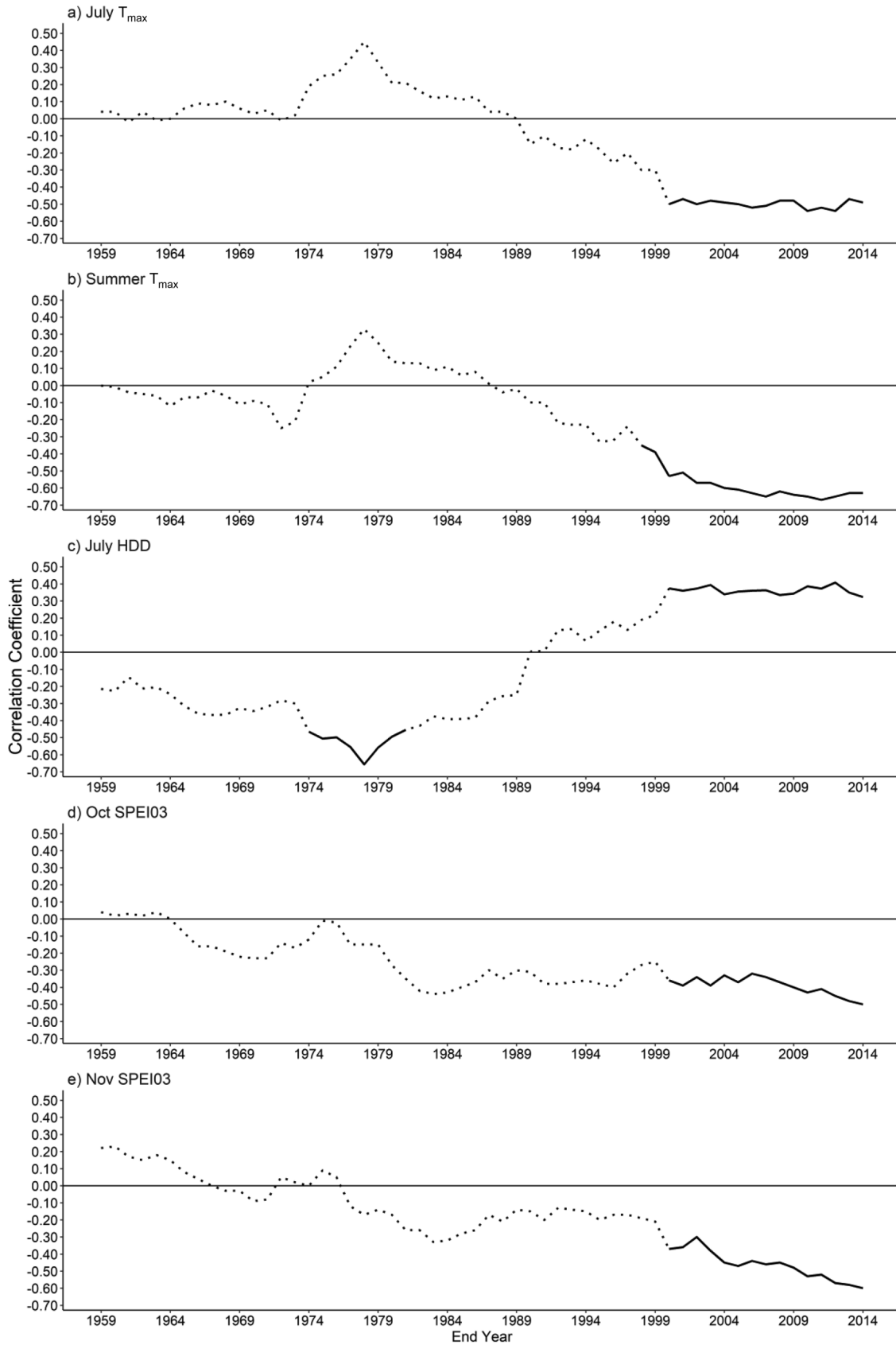
rainfall (Lynch et al. 2016). Increased potential evapotranspiration rates can create drought conditions, even in areas such as the Northeast that are projected to experience increased moisture (Cook et al. 2014). Multiple summer moisture metrics were observed to be pivotal to red oak growth; however, summer is the singular season in which projections show a decrease in precipitation in the northeastern US. This may not bode well for red oak as its growth was positively correlated with summer moisture indicators throughout the chronology. Foster et al. (2016) also project red oak growth (aboveground biomass) to respond more variably to summer moisture stress in the future as compared with other temperate species, with more growth expected in wet years, but less growth in dry years. Other work suggests that oaks may fare better than other co-occurring species during drought due to their anisohydric characteristics that enable them to regulate leaf water potential and maintain static gas exchange rates (Roman et al. 2015).

Red oak growth was also negatively correlated with fall precipitation in more recent decades. In the Northeast, the season with the greatest increase in precipitation over the last century was fall — specifically, October and November — and fall is estimated to experience precipitation increases moving forward (Janowiak et al. 2018). While it may seem counterintuitive, the negative relationship with fall precipitation in the latter half of the chronology may be connected to red oak’s physiology. Red oak is a species that retains its leaves longer (Berkley 1931) and can even retain dead leaves until the next spring (Pallardy 2010). Delayed senescence or extended retention may provide red oak with the opportunity to assimilate carbon later in the growing season if the weather is favorable (Heim 2016); however, high fall precipitation levels could reduce solar inputs needed to power photosynthesis. In addition, precipitation events in the Northeast are becoming

more extreme (Janowiak et al. 2018), so increasingly heavy autumn downpours and associated wind gusts could hasten abscission by mechanically removing leaves. This could reduce potential photosynthetic gain if leaves are lost earlier in the fall. The negative association between red oak growth and fall precipitation was not found in the central Appalachian Mountains where autumnal day length is longer (Rollinson et al. 2016), so this may be a phenomenon specific to the Northeast.

Our results from climate–growth relationships based on elevation indicate that an extended growing season may benefit red oak (Fig. 8). Growth at low-elevation sites was negatively correlated with previous October HDD (a measure of cold), similar to findings in the Hudson Valley region of New York state, where red oak showed a positive correlation with prior minimum October and current maximum October temperatures (Pederson et al. 2004). Experimental evidence in the south of red oak’s range found that, of the four deciduous species tested, red oak had the latest abscission date (Gunderson et al. 2012), suggesting that it might capitalize on increased opportunities for carbon capture if warming extended the functional growing season. Summer and fall are the seasons projected to display the greatest intensification in maximum temperature in the Northeast (Janowiak et al. 2018). Red oak growth showed a negative correlation with maximum summer temperatures, a link that was even stronger in recent decades (Fig. 10). The negative correlation with June T_{\max} for both low- and high-elevation groups was higher ($r = -0.36$, $P \leq 0.01$ for both) than with variables related to an extended growing season ($r = 0.27$ for low elevation and $r = 0.26$ for high elevation; $P \leq 0.05$; Fig. 8), suggesting that hotter summer temperatures may have a greater impact on growth than any positive benefit afforded from a longer growing season. Additionally, because tree growth exhibited a negative association with fall precipitation in

Fig. 10. Moving correlations of standardized radial growth of red oak with (a) July T_{max} , (b) summer (June, July, and August) T_{max} , (c) July HDD, (d) October SPEI03, and (e) November SPEI03. Dotted lines represent a nonsignificant relationship, and solid lines represent a significant relationship at $P \leq 0.05$. The year represents the last year of a 25-year moving window.



Can. J. For. Res. Downloaded from www.nrcresearchpress.com by USDANALBF on 10/02/20
For personal use only.

Table 1. Red oak (*Quercus rubra*) growth–climate model results from 1935 to 2014 (the entire chronology).

Adj. R^2	F ratio (model)	Prob > F (model)	Term(s)	Estimate \pm SE	F ratio (terms)	Prob > F (terms)
0.26	14.277	<0.0001***	July SPEI03	0.036 \pm 0.010	12.690	0.0006***
			June T_{max}	-0.014 \pm 0.004	15.864	0.0002***

Note: Adj. R^2 , adjusted R^2 ; SPEI03, 3-month standardized precipitation–evapotranspiration index; T_{max} , maximum monthly temperature. The P value shows the significance of the model by comparing the reduced deviance between the null model and the candidate model; it was calculated using an analysis of variance with an F statistic. Significance levels: *, $P < 0.05$; **, $P < 0.01$; ***, $P < 0.001$. For more information on variables, see Methods.

recent decades, the potential benefits of an extended growing season in the fall could be tempered by adverse influences associated with elevated fall precipitation.

While red oak sites investigated for this study have exhibited substantial growth, particularly in recent decades, there may be mounting constraints on this growth into the next century if the climate variables most associated with reduced growth (e.g., summer heat and elevated fall precipitation) become more extreme. Whether regional forests will be increasingly dominated by oak species in the future (as suggested by the CCTA) will depend on multiple factors: chiefly, the recruitment of new individuals, which may be challenging in the absence of fire, other disturbances, or artificial regeneration (e.g., Dey 2014), as well as the possible mitigating influence of an extended growing season and concomitant responses of native and introduced competitors as the climate changes. Furthermore, the dynamic effects of future changes in climate and possible increases in extreme weather events that challenge red oak growth and regeneration beyond the limits currently experienced could alter trajectories of red oak growth and survival in ways that are currently unforeseen.

Acknowledgements

We thank Anthony D'Amato and Jennifer Pontius for thoughtful suggestions regarding manuscript edits. Alan Howard and Carol Adair provided valuable statistical assistance. We thank Rebecca Rossell, Isabel Molina, Jeremy Gerber, and Elizabeth Bannar for their assistance in the field and laboratory. We also thank the Forest Ecosystem Monitoring Cooperative for their help. This research was supported by the USDA Forest Service and the USDA McIntire-Stennis Cooperative Forestry Research Program. In addition, we thank personnel from the Green Mountain National Forest, the Vermont Department of Forests, Parks and Recreation, and the Vermont towns of Essex, St. Albans, and South Burlington for access to field sites. The datasets generated for this study are available for download from The DendroEcological Network at <https://doi.org/10.18125/ba2331>.

References

Akaike, H. 1974. A new look at the statistical model identification. *IEEE Trans. Automat. Control*, **19**(6): 716–723. doi:10.1109/TAC.1974.1100705.

Altman, J., Fibich, P., Dolezal, J., and Aakala, T. 2014. TRADER: A package for Tree Ring Analysis of Disturbance Events in R. *Dendrochronologia*, **32**(2): 107–112. doi:10.1016/j.dendro.2014.01.004.

Barbaroux, C., and Bréda, N. 2002. Contrasting distribution and seasonal dynamics of carbohydrate reserves in stem wood of adult ring-porous sessile oak and diffuse-porous beech trees. *Tree Physiol.* **22**(17): 1201–1210. doi:10.1093/treephys/22.17.1201. PMID:12464573.

Berkley, E.E. 1931. Marcescent leaves of certain species of *Quercus*. *Bot. Gaz.* **92**(1): 85–93. doi:10.1086/334178.

Biondi, F., and Waikul, K. 2004. DENDROCLIM2002: A C++ program for statistical calibration of climate signals in tree-ring chronologies. *Comput. Geosci.* **30**(3): 303–311. doi:10.1016/j.cageo.2003.11.004.

Bishop, D.A., Beier, C.M., Pederson, N., Lawrence, G.B., Stella, J.C., and Sullivan, T.J. 2015. Regional growth decline of sugar maple (*Acer saccharum*) and its potential causes. *Ecosphere*, **6**(10): 1–14. doi:10.1890/ES15-00260.1.

Bunn, A.G., Jansma, E., Korpela, M., Westfall, R.D., and Baldwin, J. 2013. Using simulations and data to evaluate mean sensitivity ($\bar{\zeta}$) as a useful statistic in dendrochronology. *Dendrochronologia*, **31**(3): 250–254. doi:10.1016/j.dendro.2013.01.004.

Bunn, A., Korpela, M., Biondi, F., Campelo, F., Mérian, P., Qeadan, F., and Zang, C. 2016. dplR: Dendrochronology Program Library in R. R package version 1.6.4. Available from <http://CRAN.R-project.org/package=dplR>.

Buras, A. 2017. A comment on the expressed population signal. *Dendrochronologia*, **44**: 130–132. doi:10.1016/j.dendro.2017.03.005.

Burns, R.M., and Honkala, B.H. 1990. *Silvics of North America*. U.S. Department of Agriculture, Washington, D.C., Agriculture Handbook 654.

Cleland, D.T., Freeouf, J.A., Keys, J.E., Nowacki, G.J., Carpenter, C.A., and McNab, W.H. 2007. Ecological subregions: sections and subsections for the conterminous United States. USDA Forest Service, Washington, D.C., Gen. Tech. Report WO-76D [map on CD-ROM, presentation scale 1:3,500,000; colored; A.M. Sloan, cartographer].

Cochar, H., and Tyree, M.T. 1990. Xylem dysfunction in *Quercus*: vessel sizes, tyloses, cavitation and seasonal changes in embolism. *Tree Physiol.* **6**(4): 393–407. doi:10.1093/treephys/6.4.393. PMID:14972931.

Cook, B.I., Smerdon, J.E., Seager, R., and Coats, S. 2014. Global warming and 21st century drying. *Clim. Dynam.* **43**(9–10): 2607–2627. doi:10.1007/s00382-014-2075-y.

Cook, E.R. 1985. A time series analysis approach to tree ring standardization (dendrochronology, forestry, dendroclimatology, autoregressive process). Ph.D. Dissertation, School of Renewable Natural Resources, The University of Arizona, Tucson, Arizona.

Cook, E.R., and Kairiukstis, L.A. (Editors). 1990. *Methods of dendrochronology*. Kluwer Academic Publishers, Boston, Mass.

Cook, E.R., and Peters, K. 1981. The smoothing spline: a new approach to standardizing forest interior tree-ring width series for dendroclimatic studies. *Tree-ring Bull.* Available from <https://repository.arizona.edu/handle/10150/261038> [accessed 6 August 2018].

Cook, E.R., and Peters, K. 1997. Calculating unbiased tree-ring indices for the study of climatic and environmental change. *Holocene*, **7**(3): 361–370. doi:10.1177/095968369700700314.

Cowan, I., and Farquhar, G. 1977. Stomatal function in relation to leaf metabolism and environment. *Symp. Soc. Exp. Biol.* **31**: 471–505. PMID:756635.

Crawford, C.J. 2012. Do high-elevation northern red oak tree-rings share a common climate-driven growth signal? *Arct. Antarct. Alp. Res.* **44**(1): 26–35. doi:10.1657/1938-4246-44.1.26.

Dey, D.C. 2014. Sustaining oak forests in eastern North America: regeneration and recruitment, the pillars of sustainability. *For. Sci.* **60**(5): 926–942. doi:10.5849/forsci.13-114.

D'Orangeville, L., Maxwell, J., Kneeshaw, D., Pederson, N., Duchesne, L., Logan, T., et al. 2018. Drought timing and local climate determine the sensitivity of eastern temperate forests to drought. *Glob. Chang. Biol.* **24**(6): 2339–2351. doi:10.1111/gcb.14096. PMID:29460369.

Driscoll, C.T., Lawrence, G.B., Bulger, A.J., Butler, T.J., Cronan, C.S., Eagar, C., et al. 2001. Acidic deposition in the northeastern United States: sources and inputs, ecosystem effects, and management strategies. *BioScience*, **51**(3): 180–198. doi:10.1641/0006-3568(2001)051[0180:ADITNU]2.0.CO;2.

Driscoll, C.T., Whitall, D., Aber, J., Boyer, E., Castro, M., Cronan, C., et al. 2003. Nitrogen pollution in the northeastern United States: sources, effects, and management options. *BioScience*, **53**(4): 357–374. doi:10.1641/0006-3568(2003)053[0357:NPTNU]2.0.CO;2.

Ellmore, G.S., and Ewers, F.W. 1985. Hydraulic conductivity in trunk xylem of elm, *Ulmus americana*. *IAWA Journal*, **6**(4): 303–307. doi:10.1163/22941932-90000958.

Fei, S., Desprez, J.M., Potter, K.M., Jo, I., Knott, J.A., and Oswalt, C.M. 2017. Divergence of species responses to climate change. *Sci. Adv.* **3**(5): e1603055. doi:10.1126/sciadv.1603055. PMID:28560343.

Foster, D.R. 1992. Land-use history (1730–1990) and vegetation dynamics in central New England, U.S.A. *J. Ecol.* **80**(4): 753–771. doi:10.2307/2260864.

Foster, J.R., D'Amato, A.W., and Bradford, J.B. 2014. Looking for age-related growth decline in natural forests: unexpected biomass patterns from tree rings and simulated mortality. *Oecologia*, **175**(1): 363–374. doi:10.1007/s00442-014-2881-2. PMID:24442595.

Foster, J.R., Finley, A.O., D'Amato, A.W., Bradford, J.B., and Banerjee, S. 2016. Predicting tree biomass growth in the temperate–boreal ecotone: Is tree size, age, competition, or climate response most important? *Glob. Chang. Biol.* **22**(6): 2138–2151. doi:10.1111/gcb.13208. PMID:26717889.

- Fox, J., and Weisberg, S. 2011. An {R} companion to applied regression. 2nd edition. Sage, Thousand Oaks, Calif.
- Fritts, H.C. 1976. Tree rings and climate. Academic Press, New York.
- García-González, I., Souto-Herrero, M., and Campelo, F. 2016. Ring-porosity and earlywood vessels: a review on extracting environmental information through time. *IAWA Journal*, 37(2): 295–314. doi:10.1163/22941932-20160135.
- Gray, L.K., and Hamann, A. 2013. Tracking suitable habitat for tree populations under climate change in western North America. *Clim. Change*, 117(1–2): 289–303. doi:10.1007/s10584-012-0548-8.
- Greaver, T.L., Sullivan, T.J., Herrick, J.D., Barber, M.C., Baron, J.S., Cosby, B.J., et al. 2012. Ecological effects of nitrogen and sulfur air pollution in the US: what do we know? *Front. Ecol. Environ.* 10(7): 365–372. doi:10.1890/110049.
- Gudex-Cross, D., Pontius, J., and Adams, A. 2019. Northeastern Forest Species Composite by Percent Basal Area. FEMC. Available from <https://www.uvm.edu/femc/data/archive/project/northeast-forest-species-mapping-from-landsat/dataset/species-composite-by-percent-basal-area> [accessed 11 April 2019].
- Gunderson, C.A., Edwards, N.T., Walker, A.V., O'Hara, K.H., Campion, C.M., and Hanson, P.J. 2012. Forest phenology and a warmer climate — growing season extension in relation to climatic provenance. *Glob. Chang. Biol.* 18(6): 2008–2025. doi:10.1111/j.1365-2486.2011.02632.x.
- Hackett-Pain, A.J., Friend, A.D., Lageard, J.G.A., and Thomas, P.A. 2015. The influence of masting phenomenon on growth–climate relationships in trees: explaining the influence of previous summers' climate on ring width. *Tree Physiol.* 35(3): 319–330. doi:10.1093/treephys/tpv007. PMID:25721369.
- Heim, C. 2016. Quantitative trait loci mapping and analysis of adaptive traits in northern red oak (*Quercus rubra* L.). M.Sc. thesis, College of Agriculture, Food & Natural Resources, University of Missouri, Columbia, Missouri.
- Holmes, R.L. 1983. Computer-assisted quality control in tree-ring dating and measurement. *Tree-Ring Bull.* 43: 69–78. Available from <https://repository.arizona.edu/handle/10150/261223> [accessed 1 April 2019].
- Iverson, L.R., Thompson, F.R., Matthews, S., Peters, M., Prasad, A., Dijk, W.D., et al. 2017. Multi-model comparison on the effects of climate change on tree species in the eastern U.S.: results from an enhanced niche model and process-based ecosystem and landscape models. *Landsc. Ecol.* 32(7): 1327–1346. doi:10.1007/s10980-016-0404-8.
- Janowiak, M.K., D'Amato, A.W., Swanson, C.W., Iverson, L., Thompson, F.R., Dijk, W.D., et al. 2018. New England and northern New York forest ecosystem vulnerability assessment and synthesis: a report from the New England Climate Change Response Framework project. USDA Forest Service, Northern Research Station, Newtown Square, Penn., Gen. Tech. Rep. NRS-173. doi:10.2737/nrs-gtr-173.
- Johnson, S.E., and Abrams, M.D. 2009. Age class, longevity and growth rate relationships: protracted growth increases in old trees in the eastern United States. *Tree Physiol.* 29(11): 1317–1328. doi:10.1093/treephys/tpp068. PMID:19734547.
- Kannenberg, S.A., Maxwell, J.T., Pederson, N., D'Orangeville, L., Ficklin, D.L., and Phillips, R.P. 2019. Drought legacies are dependent on water table depth, wood anatomy and drought timing across the eastern US. *Ecol. Lett.* 22(1): 119–127. doi:10.1111/ele.13173. PMID:30411456.
- Kitin, P., and Funada, R. 2016. Earlywood vessels in ring-porous trees become functional for water transport after bud burst and before the maturation of the current-year leaves. *IAWA Journal*, 37(2): 315–331. doi:10.1163/22941932-20160136.
- Kosiba, A.M., Schaberg, P.G., Rayback, S.A., and Hawley, G.J. 2018. The surprising recovery of red spruce growth shows links to decreased acid deposition and elevated temperature. *Sci. Total Environ.* 637: 1480–1491. doi:10.1016/j.scitotenv.2018.05.010. PMID:29801241.
- Lawrence, G.B., Hazlett, P.W., Fernandez, I.J., Ouimet, R., Bailey, S.W., Shortle, W.C., et al. 2015. Declining acidic deposition begins reversal of forest-soil acidification in the northeastern U.S. and eastern Canada. *Environ. Sci. Technol.* 49(22): 13103–13111. doi:10.1021/acs.est.5b02904. PMID:26495963.
- LeBlanc, D.C. 1998. Interactive effects of acidic deposition, drought, and insect attack on oak populations in the midwestern United States. *Can. J. For. Res.* 28(8): 1184–1197. doi:10.1139/x98-098.
- LeBlanc, D.C., and Terrell, M.A. 2011. Comparison of growth–climate relationships between northern red oak and white oak across eastern North America. *Can. J. For. Res.* 41(10): 1936–1947. doi:10.1139/x11-118.
- Levesque, M., Andreu-Hayles, L., and Pederson, N. 2017. Water availability drives gas exchange and growth of trees in northeastern US, not elevated CO₂ and reduced acid deposition. *Sci. Rep.* 7: 46158. doi:10.1038/srep46158.
- Likens, G. 2016. Chemistry of bulk precipitation at Hubbard Brook Experimental Forest, Watershed 6, 1963–present. Ver 9. Environmental Data Initiative. Available from <https://doi.org/10.6073/pasta/8d2d88dc718b6c5a2183cd88ae26fb1> [accessed 20 July 2020].
- Likens, G.E., Driscoll, C.T., and Buso, D.C. 1996. Long-term effects of acid rain: response and recovery of a forest ecosystem. *Science*, 272(5259): 244–246. doi:10.1126/science.272.5259.244.
- Lovett, G.M. 1994. Atmospheric deposition of nutrients and pollutants in North America: an ecological perspective. *Ecol. Appl.* 4(4): 629–650. doi:10.2307/1941997.
- Lynch, C., Seth, A., and Thibeault, J. 2016. Recent and projected annual cycles of temperature and precipitation in the Northeast United States from CMIP5. *J. Clim.* 29(1): 347–365. doi:10.1175/JCLI-D-14-00781.1.
- Marquardt, D.W. 1970. Generalized inverses, ridge regression, biased linear estimation, and nonlinear estimation. *Technometrics*, 12(3): 591–612. doi:10.1080/00401706.1970.10488699.
- Martin-Benito, D., and Pederson, N. 2015. Convergence in drought stress, but a divergence of climatic drivers across a latitudinal gradient in a temperate broadleaf forest. *J. Biogeogr.* 42(5): 925–937. doi:10.1111/jbi.12462.
- Naidoo, R., and Lechowicz, M.J. 2001. Effects of gypsy moth on radial growth of deciduous trees. *For. Sci.* 47(3): 338–348. doi:10.1093/forests/47.3.338.
- National Atmospheric Deposition Program. 2017. NADP/NTN Monitoring. U.S. Geological Survey. Available from <http://nadp.sws.uiuc.edu/data/ntn/> [accessed 11 May 2017].
- Nehrbass-Ahles, C., Babst, F., Klesse, S., Nötzli, M., Bouriaud, O., Neukom, R., et al. 2014. The influence of sampling design on tree-ring-based quantification of forest growth. *Glob. Chang. Biol.* 20(9): 2867–2885. doi:10.1111/gcb.12599. PMID:24729489.
- NOAA National Centers for Environmental Information. 2018. Historical Palmer Drought Indices. Available from <https://www.ncdc.noaa.gov/temp-and-precip/drought/historical-palmer/> [accessed 21 November 2018].
- NOAA National Climatic Data Center. 2018. NOAA's Gridded Climate Divisional Dataset (CLIMDIV). Climate Division 2. Available from <https://www7.ncdc.noaa.gov/CDO/CDODivisionalSelect.jsp> [accessed 3 March 2018].
- Nowacki, G.J., and Abrams, M.D. 1997. Radial-growth averaging criteria for reconstructing disturbance histories from presettlement-origin oaks. *Ecol. Monogr.* 67(2): 225–249. doi:10.1890/0012-9615(1997)067[0225:RGACFR]2.0.CO;2.
- Nowacki, G.J., and Abrams, M.D. 2008. The demise of fire and “mesophication” of forests in the eastern United States. *BioScience*, 58(2): 123–138. doi:10.1641/B580207.
- Oswalt, S.N., Smith, W.B., Miles, P.D., and Pugh, S.A. 2014. Forest resources of the United States, 2012: a technical document supporting the Forest Service 2010 update of the RPA Assessment. USDA Forest Service, Washington Office, Washington, D.C., Gen. Tech. Rep. WO-91.
- Pallardy, S.G. 2010. Physiology of woody plants. Academic Press, Boston, Mass.
- Pan, C., Tajchman, S., and Kochenderfer, J. 1997. Dendroclimatological analysis of major forest species of the central Appalachians. *For. Ecol. Manage.* 98(1): 77–87. doi:10.1016/S0378-1127(97)00087-X.
- Pederson, N., Cook, E.R., Jacoby, G.C., Peteet, D.M., and Griffin, K.L. 2004. The influence of winter temperatures on the annual radial growth of six northern range margin tree species. *Dendrochronologia*, 22(1): 7–29. doi:10.1016/j.dendro.2004.09.005.
- Pederson, N., Bell, A.R., Cook, E.R., Lall, U., Devineni, N., Seager, R., et al. 2013. Is an epic pluvial masking the water insecurity of the Greater New York City Region? *J. Clim.* 26(4): 1339–1354. doi:10.1175/JCLI-D-11-00723.1.
- Prasad, A.M., and Iverson, L.R. 2003. Little's range and FIA importance value database for 135 eastern US tree species. USDA Forest Service, Northeastern Research Station, Delaware, Ohio. Available from <https://www.fs.fed.us/nrs/atlas/littlefia/index.html>.
- Prasad, A.M., Iverson, L.R., Matthews, S., and Peters, M. 2007–ongoing. A Climate Change Atlas for 134 Forest Tree Species of the Eastern United States [database]. USDA Forest Service, Northern Research Station, Delaware, Ohio. Available from <https://www.fs.fed.us/nrs/atlas/>.
- Rollinson, C.R., Kaye, M.W., and Canham, C.D. 2016. Interspecific variation in growth responses to climate and competition of five eastern tree species. *Ecology*, 97(4): 1003–1011. doi:10.1890/1515-549.1. PMID:28792601.
- Roman, D.T., Novick, K.A., Brzostek, E.R., Dragoni, D., Rahman, F., and Phillips, R.P. 2015. The role of isohydric and anisohydric species in determining ecosystem-scale response to severe drought. *Oecologia*, 179(3): 641–654. doi:10.1007/s00442-015-3380-9. PMID:26130023.
- Schaberg, P.G., DeHayes, D.H., and Hawley, G.J. 2001. Anthropogenic calcium depletion: a unique threat to forest ecosystem health? *Ecosyst. Health*, 7(4): 214–228. doi:10.1046/j.1526-0992.2001.01046.x.
- Schaberg, P.G., Miller, E.K., and Eagar, C. 2010. Assessing the threat that anthropogenic calcium depletion poses to forest health and productivity. USDA Forest Service, Pacific Northwest and Southern Research Stations, Portland, Oregon, Gen. Tech. Rep. PNW-GTR-802.
- Siemion, J., McHale, M.R., Lawrence, G.B., Burns, D.A., and Antidormi, M. 2018. Long-term changes in soil and stream chemistry across an acid deposition gradient in the Northeastern United States. *J. Environ. Qual.* 47(3): 410–418. doi:10.2134/jeq2017.08.0335. PMID:29864170.
- Soil Survey Staff, Natural Resources Conservation Service, United States Department of Agriculture. 2019. Web Soil Survey. Available from <https://websoilsurvey.sc.egov.usda.gov/> [accessed 6 September 2019].
- Speer, J.H. 2010. Fundamentals of tree-ring research. The University of Arizona Press, Tucson, Arizona.
- Speer, J.H., Grissino-Mayer, H.D., Orvis, K.H., and Greenberg, C.H. 2009. Climate response of five oak species in the eastern deciduous forest of the southern Appalachian Mountains, USA. *Can. J. For. Res.* 39(3): 507–518. doi:10.1139/X08-194.
- Stokes, M., and Smiley, T. 1968. An introduction to tree-ring dating. University of Chicago Press, Chicago, Illinois. pp. 31–46.
- Takahashi, S., Okada, N., and Nobuchi, T. 2013. Relationship between the timing

- of vessel formation and leaf phenology in ten ring-porous and diffuse-porous deciduous tree species. *Ecol. Res.* **28**(4): 615–624. doi:10.1007/s11284-013-1053-x.
- Tardif, J., and Conciatori, F. 2006a. Influence of climate on tree rings and vessel features in red oak and white oak growing near their northern distribution limit, southwestern Quebec, Canada. *Can. J. For. Res.* **36**(9): 2317–2330. doi:10.1139/x06-133.
- Tardif, J., and Conciatori, F. 2006b. A comparison of ring-width and event-year chronologies derived from white oak (*Quercus alba*) and northern red oak (*Quercus rubra*), southwestern Quebec, Canada. *Dendrochronologia*, **23**(3): 133–138. doi:10.1016/j.dendro.2005.10.001.
- Tardif, J.C., Conciatori, F., Nantel, P., and Gagnon, D. 2006. Radial growth and climate responses of white oak (*Quercus alba*) and northern red oak (*Quercus rubra*) at the northern distribution limit of white oak in Quebec, Canada. *J. Biogeogr.* **33**(9): 1657–1669. doi:10.1111/j.1365-2699.2006.01541.x.
- Thibeault, J.M., and Seth, A. 2014. Changing climate extremes in the Northeast United States: observations and projections from CMIP5. *Clim. Change*, **127**(2): 273–287. doi:10.1007/s10584-014-1257-2.
- Tyree, M., and Cochard, H. 1996. Summer and winter embolism in oak: impact on water relations. *Ann. Sci. For. INRA/EDP Sciences*, **53**(2–3): 173–180.
- Vermont Department of Forests Parks and Recreation. 2019. Annual Reports of Forest Insect and Disease Conditions in Vermont. Vermont Department of Forests Parks and Recreation, Montpelier, Vermont.
- Vicente-Serrano, S.M., Beguería, S., and López-Moreno, J.I. 2010. A multiscalar drought index sensitive to global warming: the standardized precipitation evapotranspiration index. *J. Clim.* **23**(7): 1696–1718. doi:10.1175/2009JCLI2909.1.
- Vicente-Serrano, S.M., Beguería, S., and López-Moreno, J.I. 2017. Global SPEI Database. Available from <http://spei.csic.es/database.html> [accessed 10 July 2017].
- Wang, W.J., He, H.S., Thompson, F.R., Fraser, J.S., and Dijk, W.D. 2017. Changes in forest biomass and tree species distribution under climate change in the northeastern United States. *Landsc. Ecol.* **32**(7): 1399–1413. doi:10.1007/s10980-016-0429-z.
- West, P.W. 1980. Use of diameter increment and basal area increment in tree growth studies. *Can. J. For. Res.* **10**(1): 71–77. doi:10.1139/x80-012.
- Wigley, T.M.L., Briffa, K.R., and Jones, P.D. 1984. On the average value of correlated time series, with applications in dendroclimatology and hydrometeorology. *J. Climate Appl. Meteor.* **23**(2): 201–213. doi:10.1175/1520-0450(1984)023<0201:OTAVOC>2.0.CO;2.
- Woodcock, D. 1989. Distribution of vessel diameter in ring-porous trees. *Aliso: J. Syst. Evol. Bot.* **12**(2): 287–293. doi:10.5642/aliso.19891202.05.
- Yamaguchi, D.K. 1991. A simple method for cross-dating increment cores from living trees. *Can. J. For. Res.* **21**(3): 414–416. doi:10.1139/x91-053.
- Zang, C., and Biondi, F. 2015. treeclim: An R package for the numerical calibration of proxy–climate relationships. *Ecography*, **38**(4): 431–436. doi:10.1111/ecog.01335.
- Zimmerman, M.H. 1983. Xylem structure and the ascent of sap. Springer-Verlag, New York.